NASA-CR-203029

Astron. Astrophys. 298, 934–943 (1995)

ASTRONOMY AND ASTROPHYSICS

LPI
MIS
004 921

The standard-accretion disk dynamo

G. Rüdiger[1], D. Elstner[1,2], and T.F. Stepinski[2]

[1] Astrophysikalisches Institut Potsdam, An der Sternwarte 16, D-14482 Potsdam, Germany
[2] Lunar and Planetary Institute, Houston, TX , USA

Received 8 July 1994 / Accepted 21 November 1994

Abstract. We consider the classic MHD turbulent dynamo operating in a thin, Keplerian accretion disk powered by turbulent viscous stress. The character of the turbulence is encapsulated into two constant parameters: the Shakura-Sunyaev dimensionless viscosity, α_{SS}, and the Coriolis number, $\Omega^* = 2\tau_{corr}\,\Omega$. The dependence of the total electromotive force on α_{SS} and Ω^* is derived and the dynamo-generated magnetic field is calculated in both kinematic and nonlinear regimes for a variety of different conditions in the halo. The calculations revealed that the dynamo number, $\mathcal{D}$, increases with Ω^*, but decreases with α_{SS}. The value of the critical dynamo number, $\mathcal{D}_{crit}$, depends on the magnetic diffusivity of the halo. In general, the smaller the halo diffusivity, the easier it is to generate the magnetic field in the disk.

The nonlinear models are calculated without taking into account the back-reaction of magnetic field on the structure of the disk. Such an approach is consistent providing that the magnetic Mach number, $\mathcal{M}_{mag}$, is smaller than unity. We show that $\mathcal{M}_{mag}$ is determined primarily by the value of Ω^*, and that the consistency condition $\mathcal{M}_{mag} < 1$ requires, in some cases, turbulence with relatively large Ω^*. In such a regime the dynamo number, the magnitude of the equilibrated large-scale magnetic field, as well as the ratio of the poloidal and the toroidal magnetic field strength, depend mostly on the value of α_{SS}. The generated field has a quadrupolar symmetry with respect to the equator, is mostly confined within the disk's density scale-height, and is concentrated in the radially inner part of the disk. The obtained solutions are very regular, they lack any radial reversals, and no oscillatory or chaotic behavior has been found.

Key words: accretion disks – magnetohydrodynamics – turbulence – novae, cataclysmic variables

1. Introduction

Geometrically thin, optically thick, turbulent accretion disks are believed to surround many stars. Some of them are the compact components of close binaries (X-ray binaries, cataclysmic variables), while the other are thought to be single stars (T Tauri stars). Those accretion disks must be magnetized objects, because accreted matter, whether it comes from the companion star or from a collapsing molecular cloud core, carries an embedded magnetic field. In addition, most accretion disks are hot and turbulent, thus meeting the condition for the MHD turbulent dynamo to maintain and amplify any magnetic seed field. In fact, for a disk's magnetic field to persist long enough in comparison with the disk's viscous time, it must be continuously regenerated because the characteristic diffusion time of a magnetic field is typically much shorter than the disk's viscous time. This is true for most thin accretion disks. Consequently, studying magnetic fields in thin disks is usually synonymous with studying a magnetic dynamo, a fact that is not commonly recognized in the literature.

The importance of magnetic fields generated by turbulent dynamo action in accretion disks, was first investigated by Pudritz (1981a,b) who considered analytically a steady-state solution to a dynamo equation in a Keplerian disk of constant thickness. Pudritz has found that a dynamo number scales as $\mathcal{M}_T^{-2}$, where $\mathcal{M}_T$ is a turbulent Mach number assumed to be constant throughout a disk. He calculated that if the solution inside the disk is matched to an external vacuum field, then a symmetric (quadrupole) field is the easiest to excite at a dynamo number of about 10. This result was confirmed by Stepinski & Levy (1990). An antisymmetric (dipole) solution is favored, however, if a disk is sandwiched by an exterior gas of very high electrical conductivity (Meinel et al. 1990; Rüdiger et al. 1993). Fully numerical studies of accretion disk dynamos are impaired by difficulties in properly handling the boundary conditions in thin disk geometry. Stepinski & Levy (1988) introduced a numerical method designed to overcome these difficulties; however, it proved to be inefficient when applied to accretion disks where the ratio of the radial to vertical dimensions is typically 0.01 or less. A nonlinear version of this method was recently used by Torkelsson & Brandenburg (1993) to study accretion disk dynamos. Notwithstanding the improvements, they were unable to consider disks with aspect ratios smaller than 0.1 (~vertical to radial dimension) – not small enough to be representative of any

Send offprint requests to: G. Rüdiger

class of accretion disks. Elstner et al. (1990) developed a more efficient numerical scheme that until now has been applied to galaxies, which are typically thinner than accretion disks. With the improved speed of computers this method can now be applied to accretion disks.

In this paper, we focus attention on turbulent dynamos operating in almost fully-ionized accretion disks. That eliminates from our consideration protostellar disks, which are partially ionized and thus require special treatment. We make an assumption that disk turbulence can be described by only two independent parameters, which we choose to be α_{SS} – nondimensional viscosity introduced by Shakura & Sunyaev (1973), which describes the vigor of the turbulence – and Ω^*, the Coriolis number (the inverse of the Rossby number), which is used to assess the effects of rotation on turbulence. Our magnetic dynamo is calculated for a non-magnetic disk model and we explicitly assume that the structure of the disk is not modified by the generated magnetic field.

For the numerical calculations we have chosen a fiducial case of an accretion disk around a compact star. Such a disk, referred to here as the "standard model," was first investigated by Shakura & Sunyaev (1973). It is a steady-state model based on α_{SS}-prescription of viscosity. We assume a disk surrounding a compact non-magnetic star with $1 M_\odot$ and a radius of 5×10^8 cm. The assumption of a non-magnetic central star follows from the assumed model of an accretion disk that is derived under the so-called zero-torque inner boundary condition.

The disk extends from about the star's surface to the Roche sphere, which is typically located at about a few hundred stellar radii from the compact star. The typical temperatures T are about 10^3—10^5 K depending on the location in the disk. Resistive magnetic diffusivity, η_R, given approximately by $10^{12} T^{-3/2}$ cm^2/s is 10^4—10^7 cm^2/s, much smaller than a turbulent magnetic diffusivity, η_T, which is typically of the order of 10^{12}—10^{14} cm^2/s. Thus a characteristic diffusion time, $t_{\rm diff}$, is of the order of 10^2—10^4 s, very short in comparison to the viscous time, which is of the order of years, so that a dynamically significant magnetic field can only exist due to a dynamo process.

The main purpose of the present paper is to study the linear modes and nonlinear solutions of the dynamo equation utilizing recent achievements (Rüdiger & Kitchatinov 1993) in prescribing the turbulent electromotive force (EMF) and using a 2D numerical scheme developed by Elstner et al. (1990). First, in Sect. 2, we present a brief summary of the turbulent EMF concept. In Sect. 3 we calculate turbulent EMF for the standard accretion disk. In Sect. 4 we present the results of the calculations. First the kinematic solutions are given, and we discuss how their excitation thresholds and the field configuration depend on conditions in the exterior of the disk. Then the results of nonlinear calculations are shown, followed by a discussion of the dependence on the parameters of the turbulence of the character of the generated magnetic field.

2. The turbulent EMF

The evolution of the mean magnetic field $\bar{B}$ is governed by the dynamo equation

$$\frac{\partial \bar{B}}{\partial t} = \mathrm{rot}\,(\bar{u} \times \bar{B} + \mathcal{E}), \tag{1}$$

where $\mathcal{E}$ is the turbulent electromotive force, $\mathcal{E} = \langle u' \times B' \rangle$, and $\bar{u}$ the mean velocity. We employ cylindrical polar coordinates (r, ϕ, z) and assume axisymmetry, $\partial/\partial\phi = 0$. The resistive magnetic diffusivity is negligible in comparison with the turbulent diffusion.

We assume approximate scale separation and write

$$\mathcal{E}_i = \alpha_{ij} \bar{B}_j + \eta_{ijk} \bar{B}_{j,k} + ... \tag{2}$$

The α-tensor is anisotropic, even in the case of slow rotation where the correlation time $\tau_{\rm corr}$ is short compared with the rotation period $\tau_{\rm rot}$. It is convenient to express the tensorial structure in terms of the unit vector $\hat{z} = \Omega/\Omega$, where Ω is the basic rotation, measured in terms of the Coriolis number

$$\Omega^* = 2\, \tau_{\rm corr}\, \Omega. \tag{3}$$

2.1. The α-tensor

The α-effect is mainly due to the rotational influence on the turbulence in stratified media. Density stratification as well as turbulence intensity can provide the needed inhomogeneity. We shall work here only *with pure density stratification* and assume an approximation in which only terms linear in the density gradient are included.

Kitchatinov (1991) derived the advection-type parts of the α-tensor. Rüdiger & Kitchatinov (1993) did the same with the symmetric part of the tensor. The α-effect itself is odd in the angular velocity. The chosen turbulence model was identical in both papers and it closely resembles the mixing-length theory. It describes a "quasi-isotropic" turbulence, which is isotropic over small distances and anisotropic over large ones. The latter effect is due to the density stratification. Our turbulence model closely resembles that presented in Krause & Rädler (1980). Together with the random-wave approach by Wälder et al. (1980) it is the most natural model for which a determination of α has been made so far.

Then the α-tensor has the structure

$$\alpha_{ij} = -\left[\alpha_{ij}^{(z)} \frac{\partial \log \rho}{\partial z} + \alpha_{ij}^{(r)} \frac{\partial \log \rho}{\partial r}\right] \langle u'^2 \rangle \tau_{\rm corr}, \tag{4}$$

with

$$\alpha^{(z)} = \begin{pmatrix} \frac{2}{5}\psi & 0 & 0 \\ 0 & \frac{2}{5}\psi & 0 \\ 0 & 0 & -\frac{2}{15}\psi_z \end{pmatrix} \Omega^* \tag{5}$$

and

$$\alpha^{(r)} = \begin{pmatrix} 0 & 0 & -\frac{8}{15}\psi_r \\ 0 & 0 & \frac{2}{15}\psi_\phi \\ -\frac{8}{15}\psi_r & \frac{2}{15}\psi_\phi & 0 \end{pmatrix} \Omega^*. \tag{6}$$

Due to the dominance of the vertical density gradient, the influence of the latter contribution is very small. The contribution of the vertical distribution of the turbulence intensity to the α-effect is neglected in Eq. (4). Therefore, our results only hold for a turbulent velocity field satisfying

$$\frac{\partial \langle u'^2 \rangle}{\partial z} = 0. \tag{7}$$

Currently there is no information about the true vertical stratification of the turbulence intensity in accretion disks. From the expressions given by Rüdiger & Kitchatinov (1993)

$$\psi = \frac{5}{4\Omega^{*4}} \left(\Omega^{*2} + 6 - \frac{6 + 3\Omega^{*2} - \Omega^{*4}}{\Omega^*} \arctan \Omega^* \right), \tag{8}$$

$$\psi_z = -\frac{15}{4\Omega^{*4}} \left(-\frac{10\Omega^{*2} + 12}{1 + \Omega^{*2}} + \frac{2\Omega^{*2} + 12}{\Omega^*} \arctan \Omega^* \right), \tag{9}$$

$$\psi_r = -\frac{15}{8\Omega^{*4}} \left(3 - \frac{\Omega^{*2} + 3}{\Omega^*} \arctan \Omega^* \right) \tag{10}$$

can be derived in the full Coriolis number dependence.

The given terms represent the traditional α-effect; they are all odd in Ω. Note that for large Ω^*, the function ψ runs with $1/\Omega^*$. The appearance of an off-diagonal term results from the tensorial element $G_i\Omega_j + G_j\Omega_i$ with $\boldsymbol{G}$ as the density gradient.

As usual the traditional advection effect ($\epsilon_{ijk}G_k$) is even in Ω. But, after Kitchatinov (1991), the inclusion of its full tensorial structure surprisingly provides a symmetric contribution to the α-tensor

$$\psi_\phi = \Omega^* \psi_r. \tag{11}$$

2.2. The turbulent magnetic diffusivity tensor

The turbulent magnetic diffusivity tensor exists even without basic rotation. In the absence of any anisotropies it is simply $\eta_{ijk} = \eta_T \epsilon_{ijk}$. In the presence of rotation the eddy diffusivity is decreased and η_{ijk} becomes anisotropic:

$$\eta_{ijk} = \eta_T \epsilon_{ijk} + (\eta_\parallel - \eta_T)\, \epsilon_{ijl} \hat{z}_l \hat{z}_k, \tag{12}$$

with

$$\eta_T = (\phi_1 + \phi_2)\eta_0, \quad \eta_\parallel = 2\phi_1 \eta_0 \tag{13}$$

(Kitchatinov et al. 1994), where ϕ_1 and ϕ_2 are

$$\phi_1 = \frac{3}{4\Omega^{*2}} \left(-1 + \frac{\Omega^{*2} + 1}{\Omega^*} \arctan \Omega^* \right), \tag{14}$$

$$\phi_2 = \frac{3}{2\Omega^{*2}} \left(1 - \frac{\arctan \Omega^*}{\Omega^*} \right). \tag{15}$$

The reference value for the turbulent magnetic diffusivity for slow rotation is

$$\eta_0 = c_\eta \tau_{\rm corr} \langle \boldsymbol{u}'^2 \rangle, \tag{16}$$

with the free parameter $c_\eta \leq 1$. As ϕ_1 exceeds ϕ_2, the diffusivity is enhanced in the direction of z, as can be seen by taking the curl of the diffusion term

$$\text{rot}\, \mathscr{E} = \ldots + \left[\eta_T \left(\frac{\partial^2}{\partial x^2} + \frac{\partial^2}{\partial y^2} \right) + \eta_\parallel \frac{\partial^2}{\partial z^2} \right] \tilde{\boldsymbol{B}}. \tag{17}$$

This expression is only valid in Cartesian geometry and for constant η_T and $\eta_\parallel$.

The functions ψ, ... ϕ_2 completely describe the influence of the basic rotation on the turbulent EMF. They are all derived from one and the same turbulence model. ψ and ψ_z are normalized to unity for $\Omega^* \to 0$ while the limit for the ψ_r, ...ϕ_2 is 0.5. The parameter Ω^*, which fixes the structure of the tensors, is unknown for accretion disk turbulence.

2.3. Turbulent buoyancy and diamagnetism

Buoyancy only appears as a non-linear effect. It disappears for vanishing magnetic fields. Formally it can be represented by a formal velocity, $\boldsymbol{U}^{\rm buo}$. Buoyancy results from density fluctuations due to the existence of the mean magnetic field

$$\boldsymbol{U}^{\rm buo} = -\frac{\tau_{\rm corr} \boldsymbol{g}}{C_s^2} \int \beta^2 \mathscr{H}\, q\, dk d\omega. \tag{18}$$

Here $\boldsymbol{g}$ is gravity acceleration

$$\boldsymbol{g} = C_s^2 \nabla \log \rho, \tag{19}$$

with $C_s = \sqrt{\mathscr{R}T/\mu}$ as the sound speed. β is the large-scale magnetic field normalized with its equipartition value,

$$\beta = \frac{|\tilde{\boldsymbol{B}}|}{B_{\rm eq}} \tag{20}$$

with

$$B_{\rm eq} = \sqrt{\mu \rho \langle \boldsymbol{u}'^2 \rangle}, \tag{21}$$

and $\mathscr{H}$ is a integral kernel given in Kitchatinov & Pipin (1993). The local velocity spectrum is q with

$$\langle u'^2 \rangle = \int_0^\infty q(k, \omega, \boldsymbol{x}) dk d\omega. \tag{22}$$

A "buoyancy effect" can also exist without any density fluctuations. Kitchatinov & Rüdiger (1992) found a non-linear advection term arising from the density stratification alone

$$\boldsymbol{U} = \nabla \log \rho \int \beta^2 \mathscr{H}^{\rm dens}\, q\, dk d\omega, \tag{23}$$

so that the total effect can be written as

$$\boldsymbol{U}^{\rm buo} = \nabla \log \rho \int \left(\beta^2 \mathscr{H}^{\rm dens} - \mathscr{H} \right) q\, dk d\omega. \tag{24}$$

As in thin accretion disks the density gradient is predominantly vertical, we find

$$U^{\rm buo} \simeq \frac{\tau_{\rm corr}}{H_{\rm dens}} \langle u'^2 \rangle \, \mathcal{H}^{\rm buo}(\beta) \, \hat{\boldsymbol{z}}, \tag{25}$$

integrated with the usual mixing-length representation. The density scale-height, $H_{\rm dens}$, is taken to be also the disk's half-thickness. After inserting the kernel expressions we arrive at

$$\mathcal{H}^{\rm buo} = \frac{1}{8\beta^2} \left(-\frac{3+5\beta^2}{(1+\beta^2)^2} + \frac{3}{\beta} \arctan \beta \right). \tag{26}$$

The new kernel starts with $\beta^2/5$ for weak fields and vanishes like $3\pi/(16\beta^3)$ for strong fields. This high strong-field-quenching is unexpected. The advection is always upward.

The traditional diamagnetic effect describes the effort of the inhomogeneous turbulence to expel the mean magnetic field. For slow rotation it is simply

$$U^{\rm dia} = -\frac{1}{2} \nabla \left[\tau_{\rm corr} \langle u'^2 \rangle \mathcal{H}^{\rm dia}(\beta) \right]. \tag{27}$$

The kernel $\mathcal{H}^{\rm dia}$ was given for weak and strong magnetic fields in Kitchatinov & Rüdiger (1992). For weak fields it starts with $1/3 - 2\beta^2/5$. The influence of fast rotation on the advection effect is unknown so far.

From a more general point of view the vertical flows described in this section are part of the α-effect.

2.4. The inflow

The electro-dynamically relevant radial flow, u_r, consists of various parts. Besides the standard inflow due to the turbulent viscosity, $u^{\rm visc}$, there is the diamagnetic flow, (27), as well as the magnetically induced part, $u^{\rm mag}$, of the accretion inflow due to the angular momentum transport by the Lorentz force.

With the stress tensor for turbulence and magnetism

$$T_{ij} = Q_{ij} - \frac{1}{\mu\rho} \langle B'_i B'_j \rangle - \frac{1}{\mu\rho} \bar{B}_i \bar{B}_j + \ldots \tag{28}$$

the conservation law of angular momentum can be written as

$$\frac{\partial (r^2 \rho \Omega)}{\partial t} + \mathrm{div} \left[\rho r \left(r\Omega u + t \right) \right] = 0 \tag{29}$$

with

$$t_i = T_{i\phi}. \tag{30}$$

Integration over z of the stationary form of (29) yields

$$u_r = -\frac{1}{r\Omega\Sigma} \int_{-\infty}^{\infty} \rho T_{r\phi} \, dz, \tag{31}$$

implying an accretion rate of

$$\dot{M} = \frac{1}{\Omega} \int_{-\infty}^{\infty} \rho T_{r\phi} \, dz. \tag{32}$$

The relevant terms in the stress tensor are

$$T_{r\phi} = -\nu_{\rm T} r \frac{d\Omega}{dr} - \frac{1}{\mu\rho} \bar{B}_r \bar{B}_\phi, \tag{33}$$

where the first term on the RHS describes the traditional mode of accretion by turbulent friction, while the second one gives accretion due to the Lorentz force. Hence,

$$u^{\rm mag} = \frac{1}{r\Omega H \mu\rho} \int_{-\infty}^{\infty} \bar{B}_r \bar{B}_\phi \, dz. \tag{34}$$

This magnetically driven flow, of course, also enters the dynamo equation as a non-linear feedback mechanism. The z-dependence of this flow is ignored in our model calculations.

3. The dynamo regime for the standard accretion disk

With the assumptions of Sect. 2 the turbulent EMF expressions are now to be applied to the physical conditions in an accretion disk. The vertical temperature stratification may be assumed as uniform, $T(r, z) \simeq T_{\rm c}(r)$. The standard thin-disk expression for the speed of sound C_s is

$$C_s = H \, \Omega, \tag{35}$$

where H as the disk's half-thickness. The turbulent viscosity is given by $\nu_{\rm T} = c_\nu \langle u'^2 \rangle \tau_{\rm corr}$ with $c_\nu < 1$ being an undetermined constant. Shakura & Sunyaev (1973) $\alpha_{\rm SS}$-approximation relates the turbulent viscosity to H and C_s,

$$\langle u'^2 \rangle \tau_{\rm corr} = \frac{\alpha_{\rm SS}}{c_\nu} \, C_s \, H. \tag{36}$$

Combining Eqs. (35) and (36) directly yields the turbulent Mach number $\mathcal{M}_{\rm T} = \sqrt{\langle u'^2 \rangle}/C_s$,

$$\mathcal{M}_{\rm T} = \sqrt{\frac{2}{c_\nu} \frac{\alpha_{\rm SS}}{\Omega^*}}. \tag{37}$$

Turbulence in the accretion disk must be subsonic, thus $\mathcal{M}_{\rm T} < 1$ for all feasible turbulence mechanisms. This condition establishes the lower limit on the Coriolis number

$$\Omega^* > \frac{2 \, \alpha_{\rm SS}}{c_\nu}. \tag{38}$$

Typically $\alpha_{\rm SS} < 1$, and unless $c_\nu \ll 1$ the condition (38) is not very restrictive at all.

Eqs. (35) and (36) also lead to a transparent structure of the buoyancy effect, yielding

$$U^{\rm buo} = \frac{\alpha_{\rm SS}}{c_\nu} \, \mathcal{H}^{\rm buo} \, C_s. \tag{39}$$

With Eq. (36) the complete turbulent EMF can be expressed in terms of the standard disk solution. In such a disk the vertical density stratification is given by the hydrostatic equilibrium equation

$$\frac{\partial p}{\partial z} = -\rho \Omega^2 z, \tag{40}$$

while the radial profile of density runs with $r^{-15/8}$. Hence, from (4) we can find the form of the α-tensor as

$$\alpha_{ij} = \left[\alpha_{ij}^{(z)} \frac{z}{H} + 2\alpha_{ij}^{(r)} \frac{H}{r}\right] \frac{\alpha_{SS}}{c_\nu} C_s, \tag{41}$$

and the reference value of the turbulent diffusivity is

$$\eta_0 = \frac{\alpha_{SS}}{\mathrm{Pm}} C_s H. \tag{42}$$

Here $\mathrm{Pm} = c_\nu/c_\eta$ is the magnetic Prandtl number. Within a thin disk approximation, the second term in (41) is negligible in comparison with the first term, and the α-tensor is dominated by its diagonal terms. In our numerical calculations (Sect. 4) we shall apply α, as given by (41), and η_0, as given by (42), only in the interior of the disk defined by $|z| \le H$. In the halo of the disk we set the components of the α-tensor to zero, and we use a constant turbulent diffusivity.

It is clear from Eqs. (41) and (42) that the disk dynamo theory requires H and C_s to be supplied from the solution of the standard accretion disk equations

$$H = 1.7 \times 10^8 \, \alpha_{SS}^{-1/10} \, \dot{M}_{16}^{3/20} \, r_{10}^{9/8} \tag{43}$$

in cm and

$$C_s = 1.06 \times 10^6 \, \alpha_{SS}^{-1/10} \, \dot{M}_{16}^{3/20} \, r_{10}^{-3/8} \tag{44}$$

in cm/s (cf. Frank et al. 1992). $\dot{M}_{16}$ is the accretion rate measured in units of 10^{16} g/s, and r_{10} the radial coordinate measured in units of 10^{10} cm.

In addition we must supply the accretion velocity, u^{visc}, if we want to involve the radial inflow effects on the EMF. The total accretion inflow consists of the viscous effect as well as the diamagnetic effect

$$u^{\mathrm{visc}} + u^{\mathrm{dia}} = -\left(2.7 + 0.68 \frac{\mathscr{H}^{\mathrm{dia}}}{c_\nu}\right) \times 10^4 \, \alpha_{SS}^{4/5} \, \dot{M}_{16}^{3/10} \, r_{10}^{-1/4} \tag{45}$$

in cm/s. Obviously the diamagnetic effect remains small compared with the viscous accretion flow. The accretion flow causes radial advection of magnetic field. Therefore, in an accretion disk, the inflow effects are negligible and may be omitted in the actual numerical calculations.

When invoking magnetic quenching of the turbulent EMF, one needs the radial profile of the disk's midplane density in order to calculate the radial profile of the equipartition field (46). With the Mach number $\mathscr{M}_\mathrm{T}$ introduced above we find

$$B_{\mathrm{eq}} = 634 \times \mathscr{M}_\mathrm{T} \, \alpha_{SS}^{-9/20} \, \dot{M}_{16}^{17/40} \, r_{10}^{-21/16}, \tag{46}$$

measured in Gauss. Note the strong decrease of B_{eq} with the distance from the central star.

The efficiency of buoyancy and accretion flow for the dynamo regime can be expressed by two magnetic Reynolds numbers

$$\mathrm{Rm}^{\mathrm{buo}} = \frac{U^{\mathrm{buo}} H}{\eta_0}, \qquad \mathrm{Rm}^{\mathrm{visc}} = \frac{u^{\mathrm{visc}}/r}{\eta_0/H^2}. \tag{47}$$

For the buoyancy effect one finds

$$\mathrm{Rm}^{\mathrm{buo}} \simeq \frac{\mathrm{Pm}}{c_\nu} \mathscr{H}^{\mathrm{buo}} \le 1, \tag{48}$$

while the accretion flow leads to

$$\mathrm{Rm}^{\mathrm{visc}} = \left(\frac{H}{r}\right)^2 \mathrm{Pm} \ll 1. \tag{49}$$

Except in the innermost region, we find that the accretion flow is unimportant for the dynamo, but that, generally speaking, buoyancy is important.

4. The magnetic field

In this paper we examine the dynamo-generated magnetic field in a typical accretion disk with parameters that roughly correspond to those in cataclysmic variables. Note, however, that since this work is geared toward the understanding of the basic features of accretion disk dynamos, our choice of the disk model was mostly dictated by its simplicity.

The disk in our model is located between $r_{\mathrm{in}} = 5 \times 10^9$ cm and $r_{\mathrm{out}} = 10^{10}$ cm, or between 0.5 and 1 as measured in units of 10^{10} cm. Hereafter all lengths are expressed in these units. In this range of radii the disk thickness stays within the same order of magnitude and is equal to about 0.01. Consequently, the aspect ratio of our model disk is about 1:50, much smaller than in any previous 2D numerical disk dynamo calculations. On the other hand our computational domain for kinematic calculations is $r \in (0.5, 1)$ and $z \in (0, 0.1)$. The vertical computational domain for nonlinear calculations is $z \in (-0.1, 0.1)$. Note that the vertical size of our computational domain is about an order of magnitude larger than the disk thickness. This is done to minimize an influence of arbitrary boundary conditions (imposed on the edges of the computational domain) on the solution within a disk. In general, placing the computational edge at $z = 0.1$ was enough to obtain a "clean" solution. We have encountered, however, a few cases for which solutions were influenced by the artificially imposed boundary conditions unless we expanded the vertical size of our computational domain to $z = 0.5$.

We have omitted some terms from the full turbulent EMF. We only use diagonal terms in the α-tensor because the off-diagonal terms are relatively small in a thin disk. We also still excluded terms corresponding to buoyancy, diamagnetism, and inflow. Finally, we include only the isotropic part of the turbulent magnetic diffusivity tensor and assume that $\eta_\mathrm{T} = \eta_0$. Thus, in our calculation the effect of rotational η-quenching is not yet included.

Most of the existing examples of accretion disk dynamos assume either a vacuum or a perfect conductor exterior. However, we are free to assign any magnetic diffusivity to the region extending between the disk surface and the edge of the computational domain. This is important inasmuch as the realistic conditions in a disk's halo are unknown, but, as we shall show,

the dynamo excitation threshold strongly depends on these conditions. We have parameterized these condition by the ratio

$$\varepsilon \equiv \frac{\eta^{\rm halo}}{\eta_0^{\rm disk}({\rm max})}, \tag{50}$$

where $\eta^{\rm halo}$ is the constant turbulent diffusivity in the halo, and $\eta^{\rm disk}({\rm max}) = \eta_0(r = 1)$ is the maximum diffusivity in a disk. Thus, for example, we simulate the vacuum in the halo by taking $\varepsilon = 100$, and we may approach the perfectly conducting halo by taking $\varepsilon \to 0$.

Similarly, we are free to impose any boundary conditions at the inner and outer radii of a disk. In that case, however, we have found that neither the dynamo excitation threshold, nor the character of the solution depend strongly on the particular choice of these boundary conditions. Calculations presented in this paper are done assuming a perfect conductor at $r = r_{\rm in}$ and a vacuum at $r = r_{\rm out}$.

4.1. Kinematic models

The solution of kinematic dynamo is synonymous with finding the first eigenvalue, $\mathscr{D}_{\rm crit}$, the smallest value of the dynamo number that permits magnetic field regeneration. The dynamo number, $\mathscr{D}$, is the ratio of induction to dissipation. Induction is given by the α-effect and the rotational shear, $\partial\Omega/\partial \log r$, which for a Keplerian disk is proportional to the rotation rate Ω. Note that in our model the α-effect is not radially uniform but instead grows inward: $\alpha_{\phi\phi} \propto r^{-3/8}$. The dissipation is dominated by turbulent diffusion that grows outward. η_0 changes with a radius, $\eta_0 \propto r^{3/4}$. In the case of a thin disk geometry, the customary definition of $\mathscr{D}$ is

$$\mathscr{D} = \frac{\alpha_{\phi\phi}(z = H)\,\Omega\,H^3}{\eta_0^2}. \tag{51}$$

Substituting η_0 from Eq. (42) and the α-effect from Eq. (41) yields

$$\mathscr{D} = 0.75\,\frac{\psi(\Omega^*)\Omega^*}{\alpha_{\rm SS}}\,\frac{{\rm Pm}^2}{c_\nu} = 1.48\,\frac{\psi(\Omega^*)}{c_\eta^2}\,\frac{1}{\mathscr{M}_{\rm T}^2}. \tag{52}$$

With our parameterization of the properties of the turbulence, $\mathscr{D}$ does not depend on radius. Eq. (52) demonstrates a peculiar feature of accretion disk dynamos: the most vigorous dynamo action is produced by the weakest turbulence and the sonic turbulence with $\mathscr{M}_{\rm T} = 1$ leads to the lowest dynamo number. This is because, in an accretion disk, the dynamo action is mostly due to the Keplerian differential rotation. For an important case of turbulence with a very long correlation time, $\Omega^* \to \infty$, $\psi(\Omega^*)\Omega^* \to$ constant and the dynamo number is completely determined by $\alpha_{\rm SS}$,

$$\mathscr{D} \propto \frac{1}{\alpha_{\rm SS}}. \tag{53}$$

The proportionality constant depends on the values of Pm and c_ν, but these parameters, of order unity, are believed to be independent of either $\alpha_{\rm SS}$ or Ω^*.

Table 1. Dynamo numbers as the eigenvalue of the fundamental modes for prescribed halo diffusivities. S0 is the standard quadrupole, A0 the dipole (bold: lowest value)

mode	ε =100 "vacuum"	ε =1	ε =0.01 "plasma"
S0	**6.0**	**0.8**	**0.01**
A0	160	150	70

The ratio of the magnetic field induction by the α-effect to the magnetic field induction by Keplerian rotation is given by

$$\frac{C_\alpha}{C_\Omega} \propto \psi(\Omega^*)\Omega^*\,\alpha_{\rm SS}. \tag{54}$$

This ratio is an indicator of the relative strength of toroidal and poloidal components of a generated magnetic field. Again, in the turbulent regime characterized by large Ω^*, the parameter $\alpha_{\rm SS}$ alone determines the value of C_α/C_Ω. The smaller the value of $\alpha_{\rm SS}$ the more toroidal is the generated field. The poloidal field could be of the order of the toroidal field only in a disk where $\alpha_{\rm SS} \to 1$.

The first objective of our calculations was to establish the value of $\mathscr{D}_{\rm crit}$ for a range of different conditions in the halo. We performed calculations for $\varepsilon = 100$, 1, and 0.01, to simulate the halo conditions ranging from a vacuum to a nearly perfect conductor. Table 1. shows the results of the calculations. The first case, $\varepsilon = 100$, is intended to simulate a disk surrounded by a vacuum. This is the configuration most frequently considered in the literature. Pudritz (1981b) obtained $\mathscr{D}_{\rm crit} \simeq 9$; later Stepinski & Levy (1991) calculated $\mathscr{D}_{\rm crit} \simeq 8$. Our 2D model with the simulated vacuum halo now yields the same order of magnitude: $\mathscr{D}_{\rm crit} \simeq 6$.

The second case is for $\varepsilon = 1$. It corresponds physically to the situation where diffusivity in the halo is within the same order of magnitude as the diffusivity in the disk. The third case is for $\varepsilon = 0.01$, when the diffusivity in a halo is much smaller than the diffusivity in a disk. The threshold for magnetic field generation drops to $\mathscr{D}_{\rm crit} = 0.01$. We conclude that the smaller the diffusivity in the halo, the easier it is to excite the disk dynamo.

For any particular choice of the halo diffusivity, the relation $\mathscr{D} = \mathscr{D}_{\rm crit}$ translates into a function defining the necessary conditions for the disk dynamo to operate. Figure 1 is the $\alpha_{\rm SS} - \Omega^*$ diagram, where the lines corresponding to the various halo models divide the turbulent regime for which the dynamo can work (above the line) from the regime for which the dynamo cannot work (below the line). The result is that whereas a "vacuum" model imposes a rather restrictive condition on the existence of the dynamo, the models characterized by smaller halo diffusivities are much less restrictive. In a vacuum model turbulence with $\alpha_{\rm SS} \gtrsim 0.25$ cannot maintain a dynamo regardless of how large is the Ω^*, but in the small ε models, the dynamo exist for all relevant values of $\alpha_{\rm SS}$ and for most values of Ω^*.

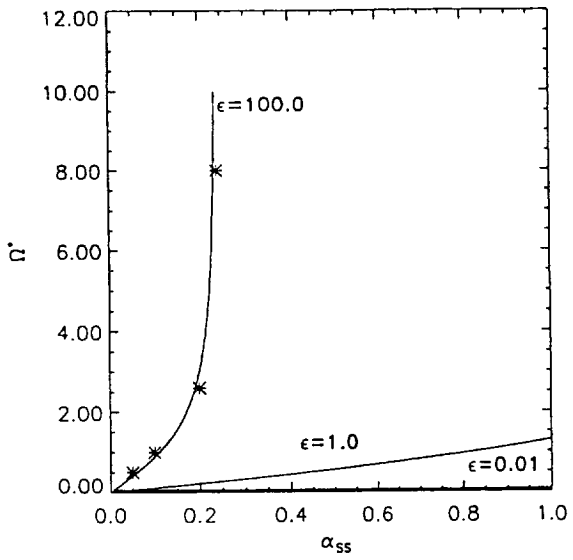

Fig. 1. Eigenvalues for dynamo excitation for various halo diffusivities. Dynamos only exist above the lines

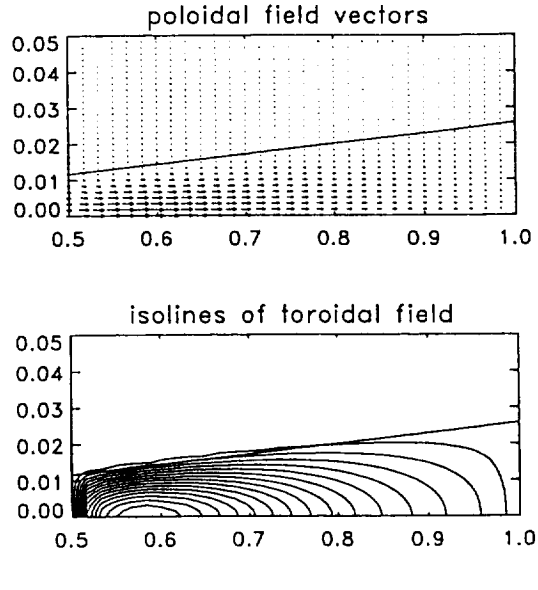

Fig. 2. The poloidal field and the toroidal field isolines of the marginal mode for a model with "vacuum halo". Note the toroidal field 10 times larger than the $\tilde{B}_r$-component ($\varepsilon = 100$)

Figures 2 and 3 show the poloidal and the toroidal field of the first normal mode calculated for the two extreme values of ε. In both cases the lowest normal mode is stationary and has a quadrupole symmetry. The field is dominated by its toroidal component and concentrated toward the disk's midplane. The degree of a field concentration toward the midplane depends on the ratio ε. In the second case ($\varepsilon = 0.01$) a field is generated in a disk as well as in the halo and the vertical distribution of the field is broader than in the first case ($\varepsilon = 100$). There are no magnetic field reversals in the radial direction in either of the two models. In the small-ε model, the field has a reversal in the vertical direction.

In both models the magnetic field achieves its maximum strength within a disk, but in a plasma halo model there is a strong secondary maximum of the field located above the disk. Figure 3 clearly illustrates the dual character of the magnetic field generated under small ε conditions: a field in a disk (generated by a combination of differential rotation and α-effect) is accompanied by a field in a halo (generated by differential rotation).

It is worth mentioning that the lowest normal mode for the disk surrounded by the true perfect conductor is dipolar rather than quadrupolar (Meinel et al. 1990). Note that solutions to our models with small ε do not yet converge to the solution of the model with perfect conductor boundary conditions.

4.2. Nonlinear models

We consider only the back-reaction of the generated magnetic field on the α-effect, ignoring any possible back-reaction of the magnetic field on the magnetic diffusivity and the large-scale Keplerian velocity field. The nonlinearity is introduced in the form of an α-quenching

$$\alpha = \frac{\alpha_0}{1+\beta^2}, \tag{55}$$

an arbitrary function of β that has a property of reducing the helicity of turbulence with increasing magnitude of a magnetic field. We acknowledge that in the turbulent regime characterized by $\Omega^* < 1$ the arbitrary formula (55) can be replaced by the expression derived from the mean-field theory (Rüdiger & Kitchatinov 1993).

We explicitly assume that the structure of a disk is not influenced by the presence of any magnetic field. Such an approach is only consistent when the field is small enough. This constraint can be expressed in terms of the magnetic Mach number as

$$\mathcal{M}_{\rm mag} = \frac{|\tilde{B}|/\sqrt{\mu\rho}}{C_s} < 1. \tag{56}$$

This condition can be used to obtain the range of the possible turbulence parameters α_{SS} and Ω^*. We rewrite (56) as $\mathcal{M}_{\rm mag} = \beta\mathcal{M}_T$, and using (37) we have

$$\beta < \sqrt{\frac{c_\nu}{2}\frac{\Omega^*}{\alpha_{SS}}}. \tag{57}$$

It gives the maximal field strength that is allowed in our concept. Using the traditional estimate $\beta \propto \mathcal{D}^{0.5}$ we find

$$\mathcal{M}_{\rm mag} \propto \frac{\sqrt{\psi(\Omega^*)}}{c_\eta}. \tag{58}$$

As ψ decreases with increasing Ω^* it is obviously more simple to fulfill $\mathcal{M}_{\rm mag} \ll 1$ for large Ω^*.

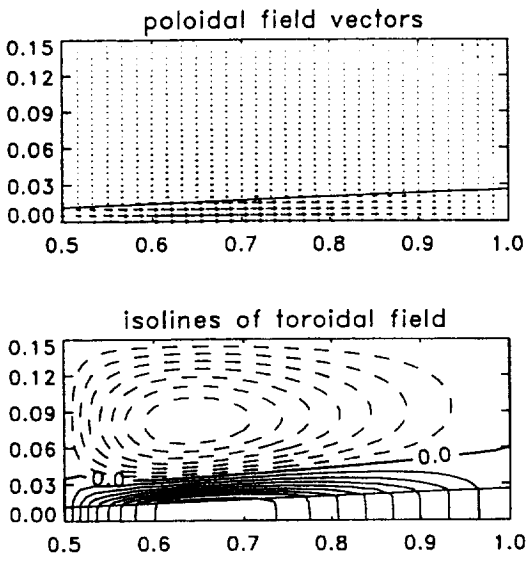

Fig. 3. The poloidal field and the toroidal field isolines of the marginal mode for a model with "plasma halo" ($\varepsilon = 0.01$)

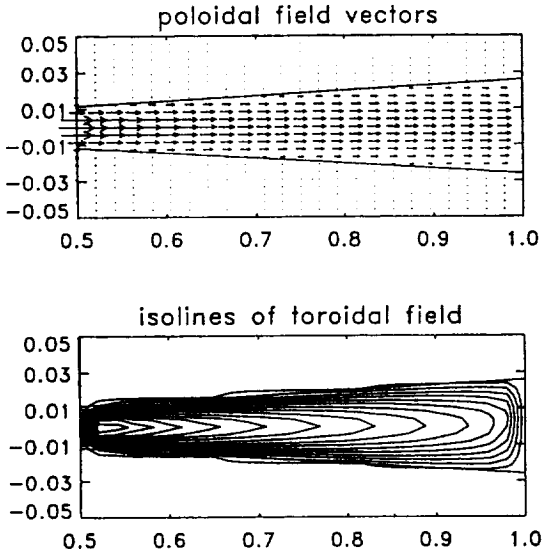

Fig. 4. The poloidal field (top) and the toroidal field isolines (bottom) for vacuum halo and large Coriolis number ($\alpha_{SS} = 0.01, \Omega^* = 10$)

In this paper we focus on calculating nonlinear models for disks with "vacuum halo." The details are presented for two models corresponding to $\alpha_{SS} = 0.01$. The first model is calculated with $\Omega^* = 10$, while the second model is calculated with $\Omega^* = 1$. The values of Ω^* had been chosen to assure that $\mathcal{M}_{mag} < 1$. Figure 4 shows the equilibrated magnetic field for the first model. The magnetic field reached equilibrium after about 70 outer rotational revolutions. The field has roughly quadrupolar symmetry and is strongly concentrated within a disk. The radial structure of the magnetic field does not resemble the structure of the corresponding normal mode, but rather reflects the radial profile of B_{eq}. The magnetic field strength exceeds the equipartition value by a factor of about 9. Because B_{eq} is a strongly decreasing function of the radius it is not surprising that the equilibrated field achieves its maximum in the innermost part of the disk.

The pitch angle $|\bar{B}_r|/|\bar{B}_\phi|$ is of the order of 0.01, yielding field lines that are almost circular. The value of $\mathcal{M}_{mag}$ is about 0.38, so the gas pressure dominates, but the magnetic pressure is significant. The generated magnetic field exerts stress; the ratio of this stress to the viscous turbulent stress is identical to the ratio $\hat{u}$ of the magnetically driven accretion flow to the normal viscous flow, which is

$$\hat{u} \equiv \left| \frac{u^{mag}}{u^{visc}} \right| = \frac{4}{3c_s\Omega^*} \frac{1}{B_{eq}^2 H} \int_0^\infty \bar{B}_r \bar{B}_\phi \, dz$$

$$\simeq \frac{2}{3} \psi(\Omega^*) \Omega^* \mathcal{M}_{mag}^2. \qquad (59)$$

For our first model $\hat{u}$ is about 0.08, so the magnetic contribution is negligible and the accretion is driven almost exclusively by turbulent viscosity.

Figure 5 shows the equilibrated magnetic field for the second model. Differences in field geometry are small compared with the first model. More important are the differences in the field strengths. The magnetic field strength exceeds the equipartition value by a factor of about 5, but the magnetic Mach number is about 0.74, and $\hat{u}$ approaches 0.3. Thus, this model is close to the limit where our theory is valid.

We also have calculated additional "vacuum halo" models. As far as the geometry of the field is concerned they are all rather similar to the examples shown in Figs. 4 and 5. Their other properties are given in Table 2.

Properties of a turbulence are encapsulated in two parameters α_{SS} and Ω^*. Ranges of these parameters appear in the first two columns of Table 2. The dynamo number shown in the fourth column depends on both α_{SS} and Ω^*, but the dependence on α_{SS} dominates. The kinetic energy of turbulent motion is measured by $\mathcal{M}_T$; it depends on both α_{SS} and Ω^*. For a given value of α_{SS}, $\mathcal{M}_T \sim 1/\sqrt{\Omega^*}$ and turbulence characterized by smaller Ω^* is more energetic. This is why the strength of a magnetic field measured in units of the equipartition value, β, given in the fifth column of Table 2, is larger for larger Ω^*.

In all calculated cases the radial profile of equilibrated magnetic field yields $\beta(r) \approx$ constant. This is illustrated in Fig. 6, where radial profiles of magnetic field strength are shown for the first three models of Table 2.

The character of the generated magnetic field is illustrated by the value of the pitch angle shown in the sixth column of Table 2. The pitch angle is proportional to α_{SS}; the smaller the α_{SS} the more toroidal is the field. The importance of the generated field on a structure of a disk is measured by $\mathcal{M}_{mag}$, shown in the seventh column of Table 2. Magnetic Mach number depends mostly on the value of Ω^*, especially for small values of α_{SS}. Note that for $\alpha_{SS} < 0.1$, models with smaller values of

Table 2. "Vacuum-halo" models: Magnetic field strength and angular momentum transport for disks with various turbulence parameters.

α_{SS}	Ω^*	$\mathcal{M}_T$	$\mathcal{D}$	β	pitch angle	$\mathcal{M}_{mag}$	$\hat{u}$	B[Gauss]	t_{rev}
0.2	10	0.20	7.1	0.8	0.16	0.16	0.01	208	46
0.1	1	0.45	6.6	0.5	0.08	0.23	0.03	402	110
0.1	10	0.14	14.1	1.8	0.06	0.25	0.03	450	46
0.01	1	0.14	66	5.3	0.007	0.74	0.27	3736	110
0.01	10	0.04	141	8.6	0.008	0.38	0.08	1729	74
0.001	1	0.04	663	18	0.0009	0.80	0.40	10206	1103
0.001	10	0.01	1417	29	0.0008	0.41	0.09	4118	735

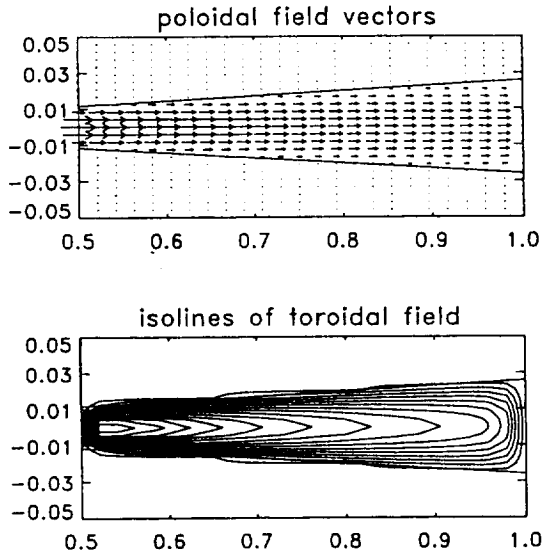

Fig. 5. The same as in Fig. 4 but for $\Omega^* = 1$

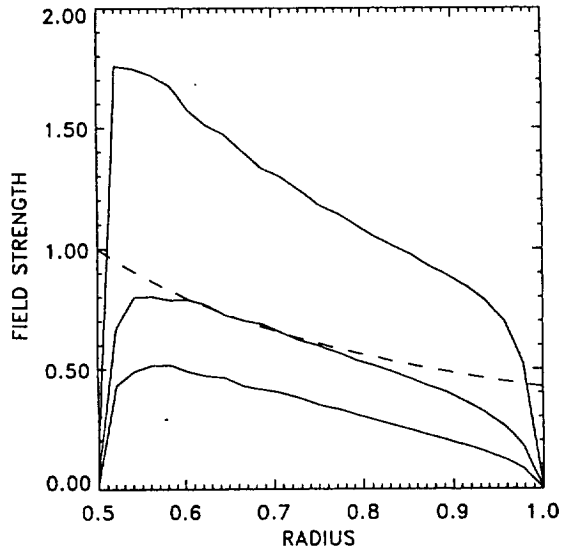

Fig. 6. The magnetic field strength of the first three models of Table 2 in units of the equipartition value at the inner boundary. The dashed line shows the equipartition field strength

Ω^* have dynamically stronger magnetic fields than those with larger values of Ω^*, despite the fact that their magnetic fields are weaker if measured in units of B_{eq}. The eighth column of Table 2 shows the values of $\hat{u}$. In most of our models the magnetic accretion flow is smaller than the turbulent viscous flow, thus the magnetic field plays no role in the accretion process.

The ninth column of Table 2 shows the maximum value of the generated magnetic field. Again, models that produce the strongest field are those at the limit of the theory. Finally, in the tenth column of Table 2 we show t_{rev}, the time needed for a magnetic field to achieve equilibrium. This time is given in units of 550 s – a Kepler revolution time at radius equal to 10^{10} cm. Note that disks characterized by larger dynamo numbers (smaller values of α_{SS}) need longer time to achieve equilibrium. This is because diffusion time, $\tau_{diff} \propto 1/\alpha_{SS}$, is longer for disks with smaller values of α_{SS}.

5. Discussion

We have discussed the existence conditions and basic properties of dynamo-generated magnetic fields in accretion disks around compact stars. We were able to study this problem in two dimensions while preserving the thin disk geometry. The major objective of our study was to find out whether a dynamo action is at all possible in a fiducial accretion disk regime and, if so, what is the character of the generated field and its role in influencing the properties of a disk. Therefore we have expressed the turbulent EMF in terms of parameters α_{SS} and Ω^*, broadly used to describe accretion disk models. Such a connection enables us to discuss the existence and the role of magnetic fields in accretion disks described by different models.

We found that in a thin Keplerian disk the sources and sinks of a magnetic field scale strongly with distance from a central star. This is a unique feature of accretion disk dynamos, and is directly related to a thin disk geometry. Dynamos in other disk-like objects like galaxies do not display this feature.

With regard to the existence of dynamo-generated magnetic fields in accretion disks we have found as follows:

- For an accretion disk surrounded by a vacuum, a turbulent dynamo can work only if the disk's turbulence is characterized by $\alpha_{SS} < 0.2$. Within a permitted range of α_{SS}, there is practically no further restriction on the value of Ω^*. The exact generation criterion is displayed in Fig. 1.
- Accretion disks surrounded by a medium with magnetic diffusivity equal or smaller than the diffusivity within a disk are much more prone to develop a working dynamo. In these models additional regeneration of magnetic field in a halo helps lower the critical dynamo number to such small levels that turbulent regimes parameterized by almost all values of α_{SS} and Ω^* lead to a successful dynamo.
- In cataclysmic variables relatively large values of α_{SS}, in the range $0.1-1$, are required to get observed outburst timescales. According to our theory, the presence or absence of dynamo generated magnetic fields in such disks may depend on the conditions in a medium around them.

Our calculations of accretion disk dynamo normal modes reveal the following:

- All disk-dynamo critical modes are stationary and have symmetric (quadrupole) equatorial symmetry. The field is predominantly toroidal and its maximum value is achieved within a disk and close to the inner edge of a disk.
- The field is confined to a disk in models with a vacuum halo, but in all other models a significant toroidal field exists just above a disk.

In this paper we restricted our nonlinear calculations to only "vacuum halo" models. We found that

- Magnetic field equilibrates after a time one to two orders of magnitude larger than a Kepler time at the outer edge of a disk. Disks with larger values of α_{SS} and smaller values of Ω^* require a longer time to equilibrate.
- The radial structure of the equilibrated field depends on the assumed nonlinearity and does not depend on the radial profile of a normal mode. Therefore, the magnetic field in units of *local* B_{eq} is uniform, the magnetic field attains the same percentage of its equipartition value everywhere in a disk. The absolute magnitude of the magnetic field is much higher in the inner part of a disk than in a outer part.
- Highest β is achieved in disks with small values of α_{SS} and high values of Ω^*. α_{SS} of the order of 0.1 leads to a magnetic field of about an equipartition strength.
- The strength of a magnetic field, as measured in units of a *local* equipartition with gas pressure, is also radially uniform; $\mathcal{M}b_{\mathcal{T}} \approx$ const. The field approaches such equilibrium for small values of Ω^*. In cataclysmic variables magnetic fields weaker than equipartition with gas pressure result.
- Regardless of how relatively strong a generated magnetic field is, its influence on angular momentum transport is small because the field is practically toroidal. The field is more likely to change the vertical structure of a disk via additional magnetic pressure.

Our results represent the first step toward understanding the nature of accretion disk dynamos. Future work will focus on nonlinear calculations for disks surrounded by a medium with diffusivity equal to or smaller than diffusivity within a disk, as well as the study of protostellar disk dynamos where the problem of low ionization of gas introduces additional complications.

Acknowledgements. A portion of this research was done while the authors were supported by the Lunar and Planetary Institute, which is operated by USRA under contract No. NASW-4574 with NASA. This is Lunar and Planetary Institute Contribution No. 835. TSF acknowledges support from NASA grant NAGW-3719.

References

Elstner, D., Meinel, R., Rüdiger, G. 1990, Geophys. Astrophys. Fluid Dyn., 50, 85
Frank, J., King, A.R., Raine, D.J. 1992, Accretion power in astrophysics, Cambridge University Press
Kitchatinov, L.L. 1991, A&A, 243, 483
Kitchatinov, L.L., Rüdiger, G. 1992, A&A, 260, 494
Kitchatinov, L.L., Pipin, V.V. 1993, A&A, 274, 652
Kitchatinov, L.L., Pipin, V.V., Rüdiger, G. 1994, Astron. Nachr., 315, 157
Krause, F., Rädler, K.-H. 1980, Mean-Field Magnetohydrodynamics and Dynamo Theory, Akademie-Verlag Berlin
Meinel, R., Elstner, D., Rüdiger, G. 1990, A&A, 236, L33
Pudritz, R.E. 1981a, MNRAS, 195, 881
Pudritz, R.E. 1981b, MNRAS, 195, 897
Rüdiger, G., Elstner, D., Schultz, M. 1993, in: The Cosmic Dynamo, IAU Symp. 157, eds. F. Krause, K.-H. Rädler and G. Rüdiger, Kluwer, Dordrecht, p. 321
Rüdiger, G., Kitchatinov, L. L. 1993, A&A, 269, 581
Shakura, N.I., Sunyaev, R.A. 1973, A&A, 24, 337
Stepinski, T.F., Levy, E.H. 1988, ApJ, 331, 416
Stepinski, T.F., Levy, E.H. 1990, ApJ, 362, 318
Stepinski, T.F., Levy, E.H. 1991, ApJ, 379, 343
Torkelsson, U., Brandenburg, A. 1993, A&A, 283, 677
Wälder, M., Deinzer, W., Stix, M. 1980, J. Fluid Mech., 96, 207

This article was processed by the author using Springer-Verlag LaTeX A&A style file version 3.